

¹⁸F-DCFPyL PET/CT in Metastatic Renal Cell Carcinoma

Geoffrey M. Currie¹, Marko Trifunovic², Jui Liu², Sang Kim³, and Howard Gurney³

¹Faculty of Science, Charles Sturt University, Wagga Wagga, Australia; ²Macquarie Medical Imaging, Macquarie University Hospital, Sydney, Australia; and ³Medical Oncology, Macquarie University, Sydney, Australia

Targeted molecular imaging with PET uses chemical ligands that are peptides specifically targeting a receptor of interest. Prostate-specific membrane antigen (PSMA) is substantially upregulated in prostate cancer but is also expressed in the neovascular tissue of several malignancies, including renal cell carcinoma (RCC). Radiolabeled peptide targets for PSMA may be helpful in detecting metastatic RCC lesions. We present a case of incidental detection of RCC metastatic disease with PSMA-targeted PET, and we explore potential use for deliberate evaluation of RCC with PSMA-targeted tracers.

Key Words: ¹⁸F-PSR; PET/CT; RCC; metastases

J Nucl Med Technol 2022; 50:282–285

DOI: 10.2967/jnmt.121.262799

Targeted molecular imaging has a foundation in the receptor principle. An important cell surface receptor is the class II membrane glycoprotein prostate-specific membrane antigen (PSMA). PSMA is the glutamate carboxypeptidase II enzyme that catalyzes *N*-acetylaspartylglutamate into glutamate and *N*-acetylaspartate. PSMA is weakly expressed on normal prostate cells but substantially upregulated in prostate cancer, particularly those of higher grade (1,2). It is well known that PSMA is also expressed in the neovascular tissue of several malignancies, including renal cell carcinoma (RCC) (1–3). PSMA is also expressed in a range of normal tissues, including the salivary glands, brain, intestines, and proximal renal tubules (3).

For PSMA radiotracers, PSMA itself is the receptor target, not the peptide. Thus, a numeric suffix generally identifies the specific peptide. PSMA-617, PSMA-11, PSMA-1007, and PSMA-I&T are commonly used. These all share the identical Lys-urea-Glu active portion of the peptide that binds to the receptor. ⁶⁸Ga-PSMA PET/CT imaging provides a high tumor-to-background ratio and so has become increasingly important in the detection and localization of prostate cancer. ⁶⁸Ga is conveniently available via a ⁶⁸Ge/⁶⁸Ga generator, which typically services a department for 6–12 mo before renewal. ¹⁸F-PSMA takes advantage of the longer half-life of 110 min and direct labeling (or Al-F chelation). ¹⁸F-PSMA is

accessible to those without the workload to justify a ⁶⁸Ga generator and those without an onsite cyclotron. Two versions are most widely reported in the literature: ¹⁸F-DCFPyL and ¹⁸F-PSMA-1007. ¹⁸F-PSMA-1007 has been reported to have less urinary excretion and bladder visualization than ⁶⁸Ga-PSMA-11 and therefore to be more useful in imaging the prostate bed (4,5). 2-(3-{1-carboxy-5-[(6-¹⁸F-fluoro-pyridine-3-carbonyl)-amino]-pentyl}-ureido)-pentanedioic acid (¹⁸F-DCFPyL), or dichlorofluorescein (DCF) pyrrolisine (PyL), is widely referred to as PSR (prostate-specific radiopharmaceutical). PSR has been reported to have less liver accumulation, which may be helpful in detecting liver metastases, although a higher distribution of dose to the kidneys and lacrimal glands was also noted (6). Importantly, ¹⁸F-PSR has been reported to have a higher accumulation than other PSMA probes in disease with a lower level of prostate-specific antigen (6).

CASE

A 70-y-old woman presented with hematuria. Twenty years previously, she had undergone laparoscopic left nephrectomy for clear cell RCC. She was found to have a bladder mass on imaging. The patient underwent a cystoscopic surgical resection of the bladder mass, and histopathologic examination confirmed metastatic clear cell RCC. The patient was referred for staging ¹⁸F-PSR PET/CT. ¹⁸F-PSR (275 MBq) was administered intravenously, with whole-body PET (vertex to thighs) and low-dose CT performed 90 min after administration.

The ¹⁸F-PSR PET/CT findings revealed no residual disease in the pelvis or abdomen (Fig. 1). However, a focus of uptake (SUV_{max}, 7.0) that exhibited a photopenic core was seen in the left parietal lobe, and a mild focus (SUV_{max}, 2.3) was seen in the right occipital lobe. There was also uptake (SUV_{max}, 6.2) associated with a large (4.2 × 4.7 × 5.7 cm) soft-tissue-density mass extending from the inferior pole of the right thyroid lobe distally into the high mediastinum; uptake associated with the mediastinal lymph nodes, including the right paratracheal (SUV_{max}, 4.9), prevascular (SUV_{max}, 6.7), and subcarinal (SUV_{max}, 5.1) regions; and uptake (SUV_{max}, 6.7) associated with the left hilar node. Physiologic uptake was noted in the left parotid and bilateral submandibular glands, whereas the right parotid gland was absent (confirmed on coregistered CT).

The ¹⁸F-PSR PET/CT findings were suggestive of moderately ¹⁸F-PSR-avid cerebral metastases involving the left

Received Jun. 25, 2021; revision accepted Sep. 10, 2021.

For correspondence or reprints, contact Geoff Currie (gcurrie@csu.edu.au).

Published online Nov. 8, 2021.

COPYRIGHT © 2022 by the Society of Nuclear Medicine and Molecular Imaging.

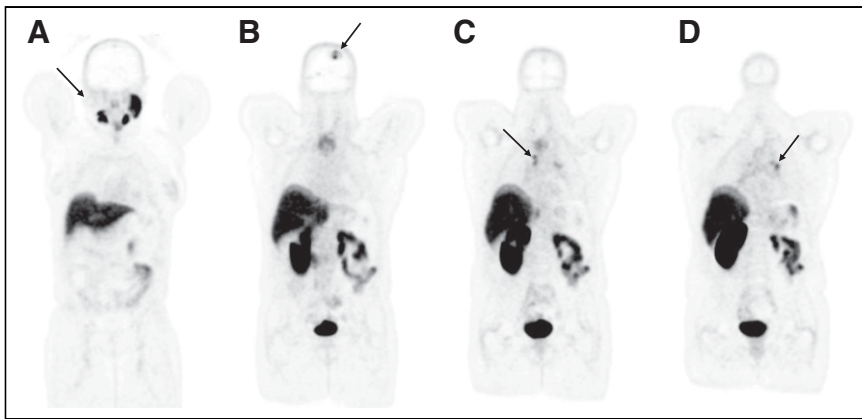


FIGURE 1. Representative coronal slices of ^{18}F -PSR PET scan. (A) Physiologic ^{18}F -PSR uptake in left parotid and bilateral submandibular glands, but absence (arrow) of right parotid gland. (B) Focal accumulation (arrow) of ^{18}F -PSR in left parietal lobe. (C) ^{18}F -PSR uptake (arrow) associated with mediastinal lymph nodes. (D) ^{18}F -PSR uptake (arrow) associated with left hilar node.

parietal and right occipital lobes, as well as of lymph nodal metastases involving the mediastinal and the left hilar nodes (Fig. 2). The moderately ^{18}F -PSR-avid right thyroid mass might have represented thyroid malignancy or further metastatic disease (Fig. 3). The patient had no symptoms of either brain metastases or mediastinal or hilar node metastases. Follow-up MRI confirmed 2 brain metastases correlating with the PET/CT. The patient underwent surgical resection of the brain metastases, and histopathologic examination confirmed metastatic clear cell RCC. She then received

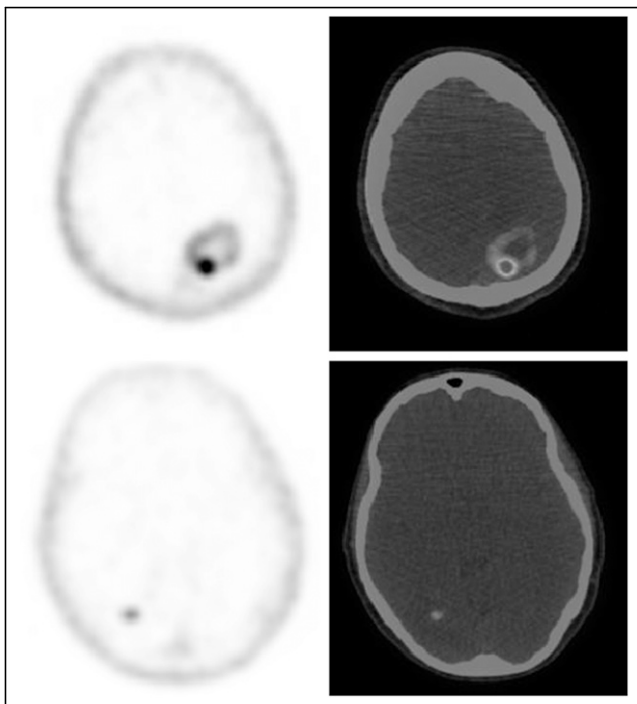


FIGURE 2. ^{18}F -PSR PET scan with transaxial slices through head demonstrating left parietal (top) and right occipital (bottom) cerebral metastases.

stereotactic radiosurgery to the surgery bed. A CT scan 2 mo later showed progression in the mediastinal nodes and thyroid, whereas MRI brain showed resolution of the brain metastases. The patient started receiving systemic therapy using lenvatinib and pembrolizumab plus a CTLA4 antibody, in a clinical trial. The patient recalled undergoing thyroid surgery some 30 years previously for a hemorrhagic cyst, but no details could be provided.

DISCUSSION

RCC is the most common primary malignancy of the kidney, with as many as 35% of patients presenting with metastatic disease at the time of diagnosis

(7). Clear cell RCC represents 75% of cases and has been targeted with PSMA imaging because of the high level of neovascularity and high degree of PSMA expression (7). Anatomic characterization (radiography, CT, and MRI) of metastatic RCC and molecular characterization with ^{18}F -FDG PET are suboptimal because of their nonspecific nature, which has further increased interest in PSMA imaging (7). PSMA is particularly helpful in detecting small metastatic lesions, although study sizes have been small. For example, one of the larger studies included 22 RCC patients, 20 with clear cell RCC, and showed that patient management was changed from the initial CT staging in 13 of 20 patients using ^{68}Ga -PSMA (8). Using ^{18}F -PSR, Rowe et al. (9) evaluated 5 clear cell RCC patients

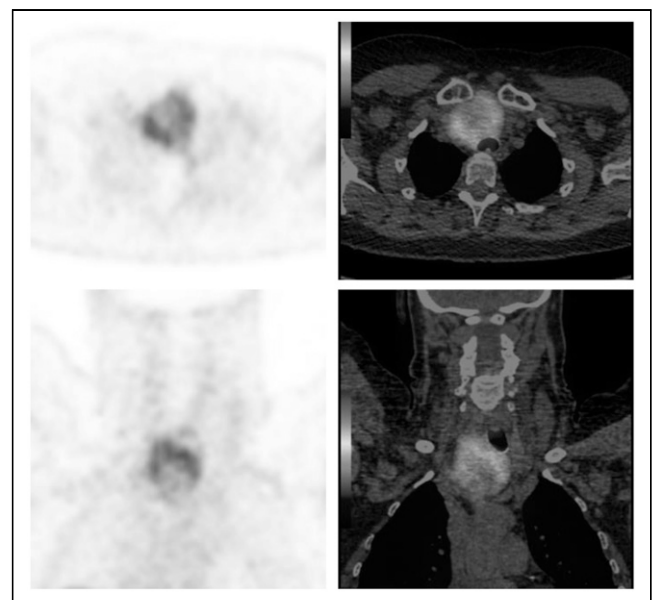


FIGURE 3. Transaxial (top) and coronal (bottom) slices of ^{18}F -PSR PET (left) with low-dose CT coregistration (right) in the right thyroid lesion.

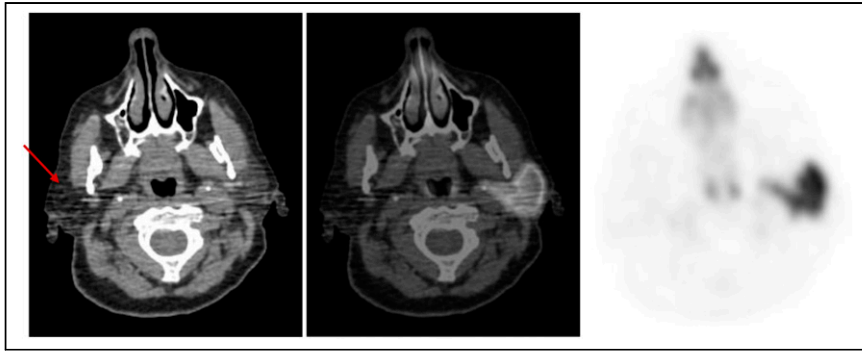


FIGURE 4. Transaxial head slices with CT (left) and ^{18}F -PSR PET (right) with low-dose CT coregistration (middle) indicating the absence of accumulation (arrow) in the right parotid salivary gland.

with 18 lesions characterized by conventional imaging and 28 on ^{18}F -PSR PET.

Brain metastases are present in 6.5% of RCC patients at the time of diagnosis (10), although reports range from 4% to 48% (11). Brain metastases are asymptomatic in patients with known RCC metastases in as many as 33% of cases (11). The presence of brain metastases is an indicator of poor prognosis (12). Given PSMA expression in RCC metastases, the detection of brain metastases in this patient was unexpected but not surprising.

Under normal conditions, both the lacrimal glands and the salivary glands accumulate PSMA-targeted radiopharmaceuticals at a high level (13,14). Indeed, decreased uptake of PSMA-targeted radiopharmaceuticals is a marker for abnormality, including inflammatory conditions (14). In this patient, despite normal ^{18}F -PSR uptake in the salivary glands, the right parotid salivary gland had an absence of uptake. Careful review of the low-dose nondiagnostic CT (Fig. 4) suggests absence of the right parotid gland, with replacement by fat tissue. This may reflect the patient's vague history of previous surgery associated with a hemorrhagic cyst, which was reported by the patient as thyroid gland but may have been salivary gland and mistakenly recalled as thyroid.

Among 12 published articles reporting an incidental accumulation of PSMA-targeted radiopharmaceuticals in the thyroid, 6 of 23 cases were malignant and 17 of 23 were benign (15). Sager et al. (16) reported 2 incidental cases of ^{68}Ga -PSMA uptake in the thyroid: the first with extensive accumulation associated with follicular thyroid carcinoma and the second with mild focal accumulation in a thyroid nodule. ^{68}Ga -PSMA imaging was suggested to be of potential value in distinguishing follicular thyroid lesions, and at a minimum it is important to be aware of potential thyroid incidentalomas to avoid misinterpretation. Verburg et al. (17) and Santhanam et al. (18) have suggested—for anti-PSMA and PSR, respectively—that PSMA expression offered a potential novel theranostic pair for advanced differentiated thyroid cancer in patients with negative radioiodine imaging results or ^{131}I resistance.

Although PSMA-targeting PET tracers are well established in prostate cancer, they have recently been reported to change management in 42% of RCC patients (19). Physiologic uptake in the parenchyma renders PSMA-targeted tracers less than ideal for primary RCC, yet they may be useful for detecting metastatic disease (20).

CONCLUSION

PSMA-targeting PET tracers provide a useful tool for both incidental and deliberate detection of metastatic RCC and may be particularly useful in the

evaluation of small lesions and those in the brain. Further clinical evaluation is recommended to explore efficacy and the potential for theranostic-pair approaches to patient management. The availability and affordability of ^{18}F -PSR provide access to PSMA-targeted PET imaging at sites without a $^{68}\text{Ge}/^{68}\text{Ga}$ generator or onsite cyclotron.

DISCLOSURE

No potential conflict of interest relevant to this article was reported.

KEY POINTS

QUESTION: Is ^{18}F -PSR useful in the evaluation of RCC metastatic disease?

PERTINENT FINDINGS: The recently Food and Drug Administration-approved ^{18}F -PSR has value for detecting metastatic RCC.

IMPLICATIONS FOR PATIENT CARE: Although ^{18}F -PSR is valuable in the armamentarium for evaluation of prostate cancer, it also has a potential role to play in RCC and other metastatic diseases that exhibit overexpression of prostate-specific antigen.

REFERENCES

- Bravaccini S, Puccetti M, Bocchini M, et al. PSMA expression: a potential ally for the pathologist in prostate cancer diagnosis. *Sci Rep.* 2018;8:4254.
- Ha H, Kwon H, Lim T, Jang J, Park SK, Byun Y. Inhibitors of prostate-specific membrane antigen in the diagnosis and therapy of metastatic prostate cancer: a review of patent literature. *Expert Opin Ther Pat.* 2021;31:525–547.
- Pozzessere C, Bassanelli M, Ceribelli A, et al. Renal cell carcinoma: the oncologist asks, can PSMA PET/CT answer? *Curr Urol Rep.* 2019;20:68.
- Ilhan H, la Fougère C, Krause BJ. PSMA-based theranostics in prostate cancer. *Urologe A.* 2020;59:617–625.
- Kesch C, Kratochwil C, Mier W, Klaus K, Giesel FL. Gallium-68 or fluorine-18 for prostate cancer imaging? *J Nucl Med.* 2017;58:687–688.
- Werner RA, Derlin T, Lapa C, et al. ^{18}F -labeled, PSMA-targeted radiotracers: leveraging the advantages of radiofluorination for prostate cancer molecular imaging. *Theranostics.* 2020;10:1–16.
- Yin Y, Campbell S, Markowski M, et al. Inconsistent detection of sites of metastatic non-clear cell renal carcinoma with PSMA-targeted ^{18}F -DCFPyL PET/CT. *Mol Imaging Biol.* 2019;21:567–573.

8. Siva S, Callahan J, Pryor D, et al. Utility of ^{68}Ga prostate specific membrane antigen positron emission tomography in diagnosis and response assessment of recurrent renal cell carcinoma. *J Med Imaging Radiat Oncol.* 2017;61:372–378.
9. Rowe SP, Gorin M, Hammers H, et al. Imaging of metastatic clear cell renal carcinoma with PSMA-targeted ^{18}F -DCFPyL PET/CT. *Ann Nucl Med.* 2015;29:877–882.
10. Ke ZB, Chen S, Chen Y, et al. Risk factors for brain metastases in patients with renal cell carcinoma. *BioMed Res Int.* 2020;2020:6836234.
11. Remon J, Lianes P, Martínez S. Brain metastases from renal cell carcinoma: should we change the current standard? *Cancer Treat Rev.* 2012;38:249–257.
12. Dudani S, de Velasco G, Wells JC, et al. Evaluation of clear cell, papillary, and chromophobe renal cell carcinoma sites and association with survival. *JAMA Netw Open.* 2021;4:e2021869.
13. van Kalmthout LW, Lam M, de Keizer B, et al. Impact of external cooling with icepacks on ^{68}Ga -PSMA uptake in salivary glands. *EJNMMI Res.* 2018;8:56.
14. Rupp NJ, Umbricht CA, Pizzuto DA, et al. First clinicopathological evidence of a non PSMA-related uptake mechanism for ^{68}Ga -PSMA-11 in salivary glands. *J Nucl Med.* 2019;60:1270–1276.
15. Bertagna F, Albano D, Giovannella L, et al. ^{68}Ga -PSMA PET thyroid incidentalomas. *Hormones (Athens).* 2019;18:145–149.
16. Sager S, Vatankulu B, Uslu L, Sönmezoglu K. Incidental detection of follicular thyroid carcinoma in ^{68}Ga -PSMA PET/CT imaging. *J Nucl Med Technol.* 2016;44:199–200.
17. Verburg FA, Krohn T, Heinzel A, Mottaghy FM, Behrendt FF. First evidence of PSMA expression in differentiated thyroid cancer using [^{68}Ga]PSMA-HBED-CC PET/CT. *Eur J Nucl Med Mol Imaging.* 2015;42:1622–1623.
18. Santhanam P, Russell J, Rooper LM, et al. The prostate-specific membrane antigen (PSMA)-targeted radiotracer ^{18}F -DCFPyL detects tumor neovasculature in metastatic, advanced, radioiodine-refractory, differentiated thyroid cancer. *Med Oncol.* 2020;37:98.
19. Raveenthiran S, Esler R, Yaxley J, Kyle S. The use of ^{68}Ga -PET/CT PSMA in the staging of primary and suspected recurrent renal cell carcinoma. *Eur J Nucl Med Mol Imaging.* 2019;46:2280–2288.
20. Lindenberg L, Mena E, Choyke P, Bouchelouche K. PET imaging in renal cancer. *Curr Opin Oncol.* 2019;31:216–221.